

# Is the Butterfly diagram due to meridional motions?

G. RÜDIGER and D. ELSTNER

Astrophysikalisches Institut Potsdam, An der Sternwarte 16, D-14482 Potsdam, Germany

Received 2002 May 10; accepted 2002 July 3

**Abstract.** The dynamo equation is solved for the solar convection zone with the given (“observed”) rotation law and positive  $\alpha$ -effect. If the latter exists in the entire convection zone the resulting dynamo shows strong toroidal field belts in the polar region migrating equatorwards. The same happens for  $\alpha$  concentrated at the bottom of the convection zone but then we get too many belts with higher amplitude. The cycle period is always too short.

Including meridional circulation which is directed equatorwards at the bottom of the convection zone (where the eddy diffusivity is reduced), the amplitude of the toroidal field grows and the butterfly diagram reaches low-latitudes. The cycle time approaches the solar value.

The dynamo regime is highly sensitive to the interplay between flow and diffusivity at the bottom of the convection zone. Stationary solutions are not very seldom.

**Key words:** solar dynamo –  $\alpha$ -effect – rotation law

## 1. Introduction

Solar dynamo theory is the explanation of the sunspot cycle. The theory is 35 years old, and yet we do not know the final solution.

Fortunately there are many more observational facts from the Sun so that we can and we must fulfill with our models a long check-list – not very long, but also not short. The full check-list contains the topics

- cycle period (22 yrs),
- parity (dipolar),
- butterfly diagram (equatorwards, low latitudes),
- amplitudes ( $|B_\phi|/|B_r| \simeq 10^{2\dots3}$ ),
- phase relations & reversals ( $B_r \cdot B_\phi < 0$ ),
- long-term stability (Maunder minimum)
- stellar statistics (e.g. of cycle times).

The last topic is also of the high relevance. Here we only mention one point; the possible cycles of young MS stars which were not included in the Wilson sample but which we now start to find with the astronomical plate archives (see Fröhlich et al., 2002). To fulfill the constraints, one needs more knowledge about the input parameters than what we have at present. Fortunately, one input parameter is now known – and this is the rotation law within the convection zone.

Correspondence to: gruediger@aip.de

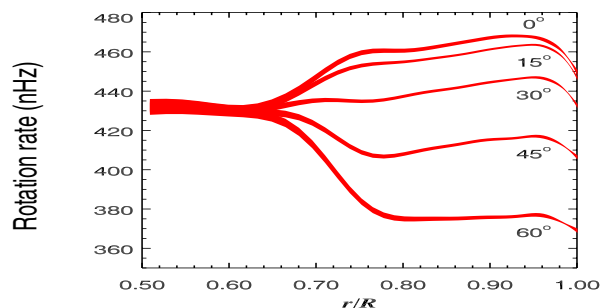


**Fig. 1.** The internal rotation law of the Sun from the inversion of SOHO data

## 2. Rotation law & meridional flow

In all our models we shall use the rotation law within the solar convection zone known by the results of helioseismology. Shortly speaking, the well-known equatorial acceleration is the result of a strong polar subrotation and a (slightly) weaker equatorial superrotation – with consequences for the dynamo regime. The solar core rotates rigidly approximately with the same angular velocity as the surface rotates at midlatitudes (Fig. 1).

The known stellar-surface rotation laws lead to the striking result that the absolute equator-pole differences of the MS stars hardly differs from star to star. This is also the result of our theory of the rotation law for stars with outer convection zones (Fig. 2, see Küker & Rüdiger, 2002). The only free pa-

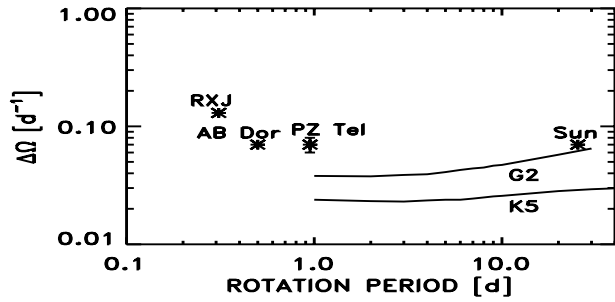


**Fig. 2.** The absolute equator-pole differences of the angular velocity observed for several stars and after the theory of Kitchatinov & Rüdiger (1999)

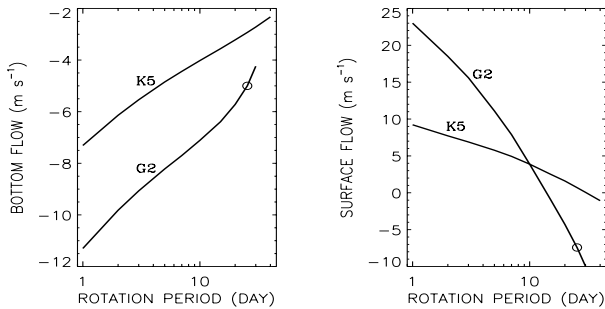


**Fig. 3.** The meridional circulation at mid-latitudes ( $45^\circ$ ) at the bottom (LEFT) and the top (RIGHT) of the convection zone for both a solar model and a K5 main-sequence star as a function of rotation period (Kitchatinov & Rüdiger 1999). The circle represents the solar case. The flow at the bottom is equatorwards (as it is the flow at the surface, there are 2 cells in radius)

rameters in the theory are the mixing-length  $\alpha$ ,  $\alpha_{MLT}$ , and the basic rotation rate of the star,  $\Omega$ .

Always such nonuniform rotation simultaneously exists with meridional flows, e.g. as then the centrifugal force cannot be written anymore as a conservative force. The flow which occurs in our simulations always at the bottom of the convection zone flows equatorwards with an amplitude of about 6 m/s (cf. Fig. 3). With  $\eta_T = 4 \cdot 10^{13} \text{ cm}^2/\text{s}$  the magnetic Reynolds number  $Rm = u^m R / \eta_T$  is of order unity so that the meridional flow only plays a minor role in the dynamo equation. Only if the magnetic eddy diffusivity is reduced by two orders of magnitude the meridional flow will strongly affect the dynamo regime (Choudhuri et al. 1995).

### 3. The $\alpha$ -effect

We are only probing dynamo models with positive(negative)  $\alpha$ -effect at the northern (southern) hemisphere. Both simulations as well as observations are suggesting such a constellation. Ossendrijver et al. (2001) have presented new simulations of the solar convection influenced by a uniform large-scale magnetic field and again found the basic result that the  $\alpha$ -component  $\alpha_{\phi\phi}$  is positive in the bulk of the convection zone and is negative in the (very thin) convection zone (Fig. 4). There is also increasing empirical evidence for negative (positive) current helicity  $\langle \mathbf{B} \text{ rot } \mathbf{B} \rangle$  at the surface (Seehafer 1990, Pevtsov et al. 1995) which after Keinigs (1983) means

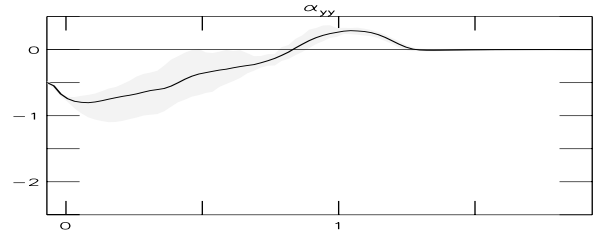


**Fig. 4.** The  $\alpha_{\phi\phi}$  component at the south pole. The top of the convection box is at the 0 on the left of the axis while the stable overshoot region begins at the 1 near the middle part of the axis.

positive(negative)  $\alpha$ -effect in the northern(southern) hemisphere (Rädler & Seehafer 1990, Rüdiger et al. 2001). Our question here is to probe the radial distribution of the (positive)  $\alpha$ -effect by comparing the resulting dynamo activity with the above-mentioned check-list.

## 4. Dynamo solutions

The dynamo equation

$$\frac{\partial \mathbf{B}}{\partial t} = \text{rot}(\mathbf{u} \times \mathbf{B} + \alpha \circ \mathbf{B} - \eta_T \text{rot } \mathbf{B}) \quad (1)$$

is solved with  $\mathbf{u}$  as the given solar rotation law. The eddy diffusivity,  $\eta_T$ , is assumed as homogeneous within the entire convection zone while the solar core is considered as a perfect conductor. The  $\alpha$ -effect always runs with  $\cos \theta$ , its radial dependence is assumed to be unknown. Only the kinematic theory is considered. If the angular velocity,  $\Omega$ , has only a radial gradient, then the cycle time turns out to be of order  $\tau_{\text{cyc}} \approx 0.26 DR / \eta_T$  with  $D$  as the depth of the convection zone. The value  $\eta_T \approx 10^{12} \text{ cm}^2/\text{s}$  is thus a reference value which would lead to the cycle time of 10 yrs.

### 4.1. Distributed dynamos

Let us apply the “observed” rotation law to Eq. (1) and assume the  $\alpha$ -effect as depth-independent. The characteristic form of the butterfly diagram is given in Fig. 5.

We can only find a radial drift of the toroidal field belts rather than a latitudinal one (Steenbeck & Krause 1969, Köhler 1973, Küker et al. 1999). The parity of the solution is dipolar, but the toroidal magnetic amplitudes are too weak ( $\approx 10$  in units of the poloidal pole field) and also the phase relation does not fit the observations. Also the cycle time is too short (see Fig. 6).

We can improve the problems with the field amplitudes and the cycle time if the  $\alpha$ -effect is concentrated to a thin layer at the bottom of the convection zone. Then the amplitude ratio exceeds values of 200 but we always get more magnetic belts than we need (Fig. 7). Also, of course, the butterfly diagram is seated at much too high latitudes and will never reach the low latitudes which are necessary to reflect the solar observations correctly.

Summing up, simple kinematic  $\alpha\Omega$ -dynamos working in the convection zone with positive  $\alpha$ -effect and the real rotation law are not able to fulfill the main constraints of our above check-list.

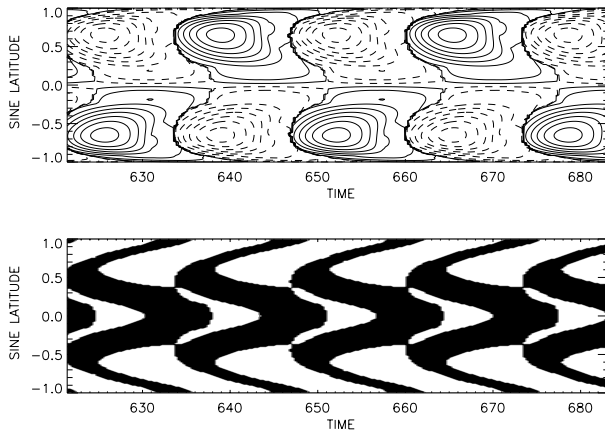


**Fig. 5.** Butterfly diagram (top) and  $B_r \cdot B_\phi$ -relation (bottom) for dynamo models with the solar rotation law, positive  $\alpha$ -effect, with eddy diffusivity of  $10^{11} \text{ cm}^2/\text{s}$  and with thick outer  $\alpha$ -layer,  $\alpha = 14 \text{ cm/s}$ , and  $u_0 = 0$  for a run with  $\alpha$ -quenching (Küker et al. 2001)

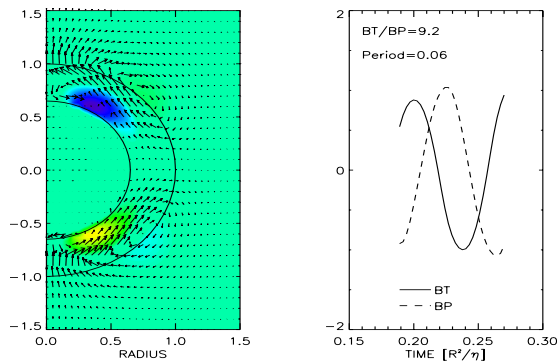


**Fig. 6.** The reference dynamo model with  $\alpha$ -effect in the convection zone (0.7...1). The cycle time is given in units of the diffusion time (33 yrs for  $\eta_T = 5 \cdot 10^{12}$ )

#### 4.2. Advection-dominated dynamos

The inclusion of the meridional flow  $u^m$  has a strong impact in the mean-field dynamo when the eddy diffusivity  $\eta_T$  is so low that the magnetic Reynolds number  $R_m = u^m R / \eta_T$  reaches values of the order of  $10^3$ . As a consequence, depending on the localization of the dynamo wave, one expects a strong modification of the dynamo regime. This possibility has been a subject of intense numerical investigation (Dikpati & Charbonneau 1999, Küker et al. 2001, Bonanno et al. 2002) where it has been shown that solutions with high magnetic Reynolds number provide correct cycle period, butterfly diagrams, magnetic phase relations with a *positive*  $\alpha$ -effect in the northern hemisphere.

We start with a model where the (positive)  $\alpha$ -effect exists through the whole convection zone. In Table 1 the results are given. Suffix A denotes (dipolar) solutions with antisymmetry with respect to the equator and suffix S denotes (quadrupolar) solutions with symmetry with respect to the equator. The drift amplitude varies between 2 cm/s and 10 cm/s but almost always the quadrupole solution occurs with the lowest  $\alpha$ -effect amplitude. Also the oscillation period of

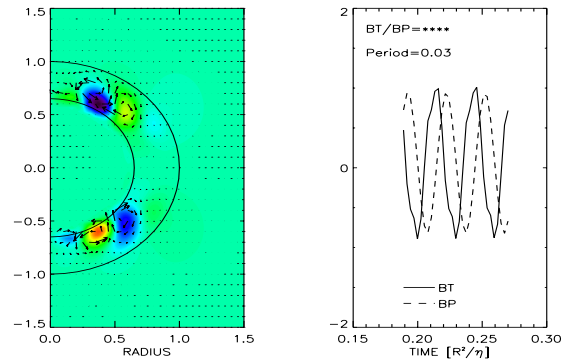


**Fig. 7.**  $\alpha$ -effect only at the bottom (0.7...0.8). Note the increase of the toroidal field amplitude

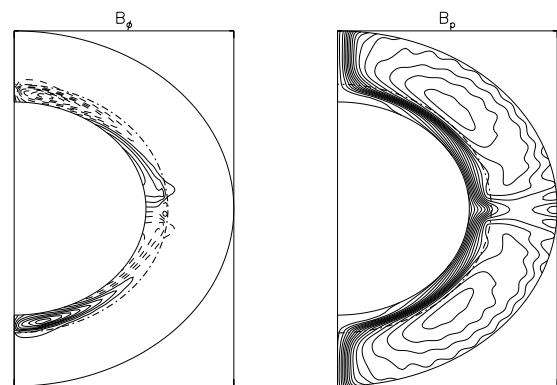


**Fig. 8.** Advection dominated dynamo:  $\alpha$ -effect in the entire convection zone: Toroidal (left) and poloidal (right) antisymmetric (dipolar) field configuration for  $\eta_T = 10^{11} \text{ cm}^2/\text{s}$ ,  $u_m = 3 \text{ m/s}$ . The solution is plotted as  $B_\phi$  isocontours and poloidal magnetic field lines. Solid contours corresponds to positive toroidal field and dashed contours to negative toroidal field Bonanno et al. (2002)

the linear dynamo is given: the dipole cycles are larger than the quadrupole cycles by a factor of 2. As usual, with the small values of eddy diffusivity which we have used, the cycle period becomes too long compared with the 22 years of the Sun. As we know from the theory of the overshoot dynamo the inclusion of nonlinear feedback of the magnetic field (via  $\alpha$ -quenching) the periods can be reduced to more realistic values (Rüdiger & Brandenburg 1995).

The toroidal field belts are concentrated at the bottom of the convection zone, and the poloidal field exhibits a rather small-scaled structure close to the surface (Fig. 8). The toroidal field belts are migrating equatorwards but, the maximum field strengths exist in the polar region.

The situation is completely changed if the  $\alpha$ -effect is located only at the bottom of the convection zone. We have worked with a thin  $\alpha$ -layer between  $x = 0.7$  and  $x = 0.8$ . In Table 2 one finds the eigenvalues for this model. Now and only now always the dipolar parity has the lowest values. At the same time, the meridional flow advects the field equatorwards producing a butterfly diagram of the observed type (Fig. 9).

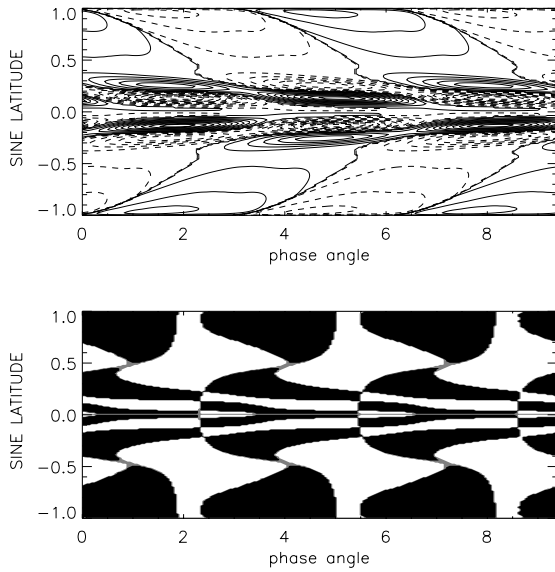


**Fig. 9.** Advection dominated dynamo:  $\alpha$ -effect at the bottom (0.7... 0.8). The flow amplitude is 5 m/s. The  $\eta_T$  is  $10^{11}$  cm<sup>2</sup>/s throughout the convection zone (Bonanno et al. 2002)

**Table 1.** Critical  $\alpha$ -values (cm/s) and periods  $P$  (yrs) for models with  $\alpha$ -effect in the entire convection zone. Bold is used when the dipolar solution has the smallest  $\alpha$ -value.

$u^m$	$\alpha_A$	$P_A$	$\alpha_S$	$P_S$
2.0	<b>0.90</b>	$\infty$	1.28	131
3.0	1.83	82	1.70	83
6.0	2.46	51	2.17	54
10.0	3.93	37	3.45	41

**Table 2.** Critical  $\alpha$ -values (cm/s) and periods (yrs) for a very thin  $\alpha$ -layer located between  $x_\alpha = 0.7$  and  $x_\beta = 0.75$  for various values of the flow (m/s), for both antisymmetric and symmetric field configurations and for  $\eta_T = 10^{11}$  cm<sup>2</sup>/s.

$u^m$	$\alpha_A$	$P_A$	$\alpha_S$	$P_S$
1	<b>0.43</b>	$\infty$	1.14	90.8
2	<b>1.37</b>	$\infty$	1.83	$\infty$
3	<b>4.36</b>	74	4.94	64
5	<b>7.53</b>	38	8.46	35
7	<b>9.22</b>	34	9.65	33
12	<b>16.61</b>	23	16.77	23

Fig. 10 presents an example with  $\eta_T = 10^{12}$  cm<sup>2</sup>/s. The toroidal field is concentrated at the bottom of the convection zone, where, however, the highest field amplitudes occur in the polar regions.

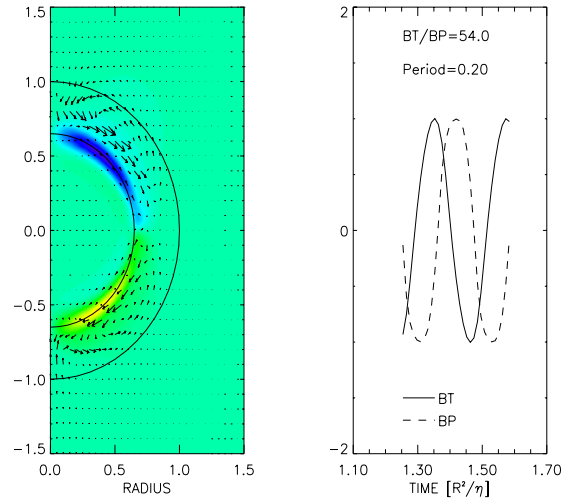


**Fig. 10.** Advection dominated dynamo:  $\alpha$ -effect at the bottom (0.7... 0.8). The flow amplitude is 5 m/s. The  $\eta_T$  is  $10^{12}$  cm<sup>2</sup>/s in the bulk of the convection zone but it is smaller at its bottom. The core has an eddy diffusivity of  $2 \cdot 10^{10}$  cm<sup>2</sup>/s

## References

- Abramenko, V.I., Wang, T., Yurchishin, V.B.: 1996, *SoPh* 168, 75
- Bonanno, A., Elstner, D., Rüdiger, G., Belvedere, G.: 2002, *A&A*, accepted (astro-ph/0204308)
- Brandenburg, A., Schmitt, D.: 1998, *A&A* 338, L55
- Choudhuri, A.R., Schüssler, M., Dikpati, M.: 1995, *A&A* 303, L29
- Dikpati, M., Charbonneau, P.: 1999, *ApJ* 518, 508
- Dikpati, M., Gilman, P.A.: 2001, *ApJ* 559, 428
- Dikpati, M., Gilman, P.A.: 2001, in: Mathys, et al. (eds.), *Magnetic Fields across the Hertzsprung-Russell Diagram*
- Fröhlich, H.-E., Tschäpe, R., Rüdiger, G., Strassmeier, K.G.: 2002, *A&A*, submitted
- Fröhlich, H.-E., Tschäpe, R., Rüdiger, G., Strassmeier, K.G.: 2002, *Poster-Proceedings of the 1st Potsdam Thinkshop*
- Hale, G.E.: 1927, *Nature* 119, 708
- Keinigs, R.K.: 1983, *PhFl* 76, 2558
- Kitchatinov, L.L., Rüdiger, G.: 1999, *A&A* 344, 911
- Köhler, H.: 1973, *A&A* 25, 467
- Küker, M., Rüdiger, G.: 2002, *Poster-Proceedings of the 1st Potsdam Thinkshop*
- Küker, M., Rüdiger, G., Schultz, M.: 2001, *A&A* 374, 301
- Ossendrijver, M., Stix, M., Brandenburg, A.: 2001, *A&A* 376, 713
- Pevtsov, A.A., Canfield, R.C., Metcalf, T.R.: 1995, *ApJ* 440, L109
- Rädler, K.-H., Seehafer, N.: 1990, in: Moffatt, Tsinober (eds.), *Topological Fluid Mechanics*
- Rüdiger, G., Brandenburg, A.: 1995, *A&A* 296, 557
- Rüdiger, G., Pipin, V.V., Belvedere, G.: 2001, *SoPh* 198, 241
- Seehafer, N.: 1990, *SoPh* 125, 219
- Steenbeck, M., Krause, F.: 1969, *AN* 291, 49